Biochemistry

© Copyright 2003 by the American Chemical Society Volume 42, Number 22 June 10, 2003

Accelerated Publications

New Phases of Phospholipids and Implications to the Membrane Fusion Problem†

Lin Yang,‡ Lai Ding,§ and Huey W. Huang*,§

National Synchrotron Light Source, Brookhaven National Laboratory, Upton, New York 11973, and Department of Physics and Astronomy, Rice University, Houston, Texas 77251

Received March 25, 2003; Revised Manuscript Received April 30, 2003

ABSTRACT: Membrane fusion is a ubiquitous process in eukaryotic cells. When two membranes fuse, lipid must undergo molecular rearrangements at the point of merging. To understand how lipid structure transitions occur, scientists studied the phase transition of lipid between the lamellar (L_α) phase and the inverted hexagonal (H_{II}) phase, based on the idea that lipid must undergo a similar rearrangement as in fusion. However, previous investigations on the system of dioleoylphosphatidylcholine (DOPC) and dioleoylphosphatidylethanolamine (DOPE) did not reveal intermediate phases between the L_α and H_{II} phases. Recently, we found a rhombohedral phase of diphytanoylphosphatidylcholine between its L_α and H_{II} phases using substrate-supported samples. Here we report the observation of two new phases in the DOPC−DOPE system: a rhombohedral phase and a distorted hexagonal phase. The rhombohedral phase confirms the stalk hypothesis for the $L_\alpha-H_{II}$ transition, but the phase of stable stalks exists only for a certain range of spontaneous curvature. The distorted hexagonal phase exists only in a lipid mixture. It implies that lipids may demix to adjust its local spontaneous curvature in order to achieve energy minimum under stress.

In cell membranes, lipids form thermodynamically stable bilayers that are the universal basis for membrane structure. These same lipids, however, must undergo drastic conformation transitions during membrane fusion. What drives the lipid structural changes is a key question at the heart of the membrane fusion problem (*1*, *2*). To find the answer, scientists have extensively investigated lipid systems undergoing the transitions between the lamellar (L_α) phase and the hexagonally packed cylindrical (H_{II}) phase (*3*−*8*), searching for structures that might resemble presumed intermediate states of fusion. This connection would help to clarify the free energy pathway for the fusion process. Recently, a stable lattice of lipid fusion structure, a rhombohedral phase, was found in an obscure lipid, diphytanoylphosphatidylcholine (DPhPC)[1] (*9*, *10*), between its L_α and H_{II} phases. That raised the question as to why the same phase was not found in the system of dioleoylphosphatidylcholine (DOPC)−dioleoylphosphatidylethanolamine (DOPE) that has been extensively investigated (*4*−*6*, *11*, *12*). In this paper

† This work was supported by NIH Grants GM55203 and RR14812 and by the Robert A. Welch Foundation (to H.W.H). L.Y. is supported by a LDRD grant from the Brookhaven National Laboratory. This research was carried out in part at beamline X21 of the National Synchrotron Light Source, Brookhaven National Laboratory, which is supported by the Division of Materials Sciences and Division of Chemical Sciences, U.S. Department of Energy, under Contract DE-AC02-98CH10886.

* To whom correspondence should be addressed. Telephone: (713) 348-4899. Fax: (713) 348-4150. E-mail: hwhuang@rice.edu.

‡ Brookhaven National Laboratory.

§ Rice University.

[1] Abbreviations: DPhPC, 1,2-diphytanoyl-*sn*-glycero-3-phosphatidylcholine; DOPC, 1,2-dioleoyl-*sn*-glycero-3-phosphatidylcholine; DOPE, 1,2-dioleoyl-*sn*-glycero-3-phosphatidylethanolamine; TFE, trifluoroethanol.

10.1021/bi0344836 CCC: $25.00 © 2003 American Chemical Society
Published on Web 05/15/2003

we show the observation of a rhombohedral phase and a distorted hexagonal phase in the DOPC−DOPE system. This finding sheds new light on lipid structural transitions.

Membrane fusion is a ubiquitous process for the distribution and redistribution of biomolecules in cells and between cells. As such, its occurrence requires special proteins and is subject to selective control. Initially, there was a question as to whether the mechanism of fusion is basically lipidic in nature (the lipidic pore hypothesis) with proteins playing a catalytic role or whether proteins play the dominant role (the protein pore hypothesis). Accumulated evidence has led to a generally accepted conceptual framework that fusion events occur by lipid molecular rearrangements that, though clearly modified by the presence of proteins, can be studied and defined in their essence through the use of appropriate model membrane systems (*1*). The main task of the protein catalysts is to provide specificity to the fusion event by limiting it in time and space within the cells and to reduce energy barriers to the intermediate and the final states of bilayer fusion (*2*).

According to the widely accepted model for membrane fusion (*1, 2*), the first intermediate state of two fusing lipid bilayers is the merging of two apposing monolayers, resulting in an hourglass-shaped structure, called a stalk, where the merged monolayer bends toward the lipid headgroups, described as a negative curvature. This process is also expected to occur in the transition from the lamellar phase to the inverted hexagonal phase. Thus it is generally believed that fusion membranes contain lipids endowed with a spontaneous negative curvature, such as DOPE or mixtures of DOPE and DOPC that are well-known for their inverted hexagonal phases. Indeed, much of the conceptual framework for the membrane fusion problem has derived from the studies of the $L_\alpha-H_{II}$ transitions. However, the experimental data of the $L_\alpha-H_{II}$ transitions alone did not provide sufficient constraints for the possible intermediate states of fusion (*13*−*15*). In fact, the absence of an intermediate state or phase between the L_α and H_{II} phases of the DOPC−DOPE system was puzzling, as if the theoretical understanding were amiss. Our work was motivated to resolving this puzzle.

MATERIALS AND METHODS

1,2-Dioleoyl-*sn*-glycero-3-phosphatidylcholine (DOPC) and 1,2-dioleoyl-*sn*-glycero-3-phosphatidylethanolamine (DOPE) were purchased from Avanti Polar Lipids (Alabaster, AL) and used as delivered. DOPC−DOPE mixtures were deposited from an organic solution on flat Si, Si_3N_4, or SiO_2 substrates. The lipid amount was about 0.5 mg/cm^2. The organic solvent was a trifluoroethanol (TFE)−chloroform mixture. The ratio of TFE to chloroform was varied to give a uniform spreading on the substrate (*16*). The organic solvent was then removed in a vacuum or evaporated in open air. Afterward, the deposit was hydrated with saturated water vapor at room or higher (∼35 °C) temperature.

X-ray diffraction was measured both at Rice with a laboratory X-ray generator and at beamline X21 of the National Synchrotron Light Source (NSLS), Brookhaven National Laboratory (Upton, NY). At Rice, a point source of Cu Kα radiation (operating at 35 mA/40 kV) was first Ni filtered and then focused by a pair of spherically bent X-ray mirrors (Charles Supper Co., Natick, MA). The mirrors were Ni-coated to further reduce the Kβ radiation. The sample was oriented at a small incident angle (<1°) with respect to the plane of the substrate. X-ray diffraction was collected using a Siemens X1000 multiwire proportional chamber (512 × 512 pixels; Bruker AXS Inc., Madison, WI) at the sample-to-detector distance of 21.54 cm. The distance was measured using sucrose powder as a calibration standard. The experimental setup at beamline X21 of the NSLS was similar to the one described in Yang and Huang (*10*) with some improvements, including (1) a rapid in-plane rotation of the substrate to ensure the (in-plane) uniformity of the sample and (2) an improvement on the heaters to allow for higher sample temperatures. The results obtained from the two sources are consistent. The diffraction patterns reported here were obtained from the NSLS.

The temperature of the sample and the relative humidity (RH) of its surrounding air were controlled inside a sample chamber (*10*). The sample was attached to a temperature-controlled aluminum disk. Directly facing the sample surface was a water reservoir, where the water temperature was adjusted to vary the relative humidity inside the sample chamber. A temperature transducer (AD590, Analog Devices) and a relative humidity sensor (HC-600, Ohmic, MD) were mounted close to the sample to monitor the sample condition. The outputs from the sensing elements were fed to PID feedback control circuits, which in turn powered two sets of Peltier modules (Melcor, NJ), one for heating or cooling the sample and another for the water reservoir. The chamber was covered by a double-layered insulating wall including kapton windows for the passage of X-rays. Between the two layers a resistive heating coil maintained the surface temperature of the chamber above that of the sample so as to avoid water condensation on the kapton windows. During the measurement, the sample mount was shifted frequently so that different parts of the sample were exposed to X-rays. This was to avoid radiation damage to the sample. An X-ray attenuator (a stack of aluminum foils) was used to reduce the intensities of the first few orders of reflection normal to the substrate, so as to avoid saturating the pixels on the CCD detector.

The experiment was performed by varying the humidity in steps of 3% RH at a fixed temperature. Five minutes was allowed for the sample to change to a new *T*/RH setting. The exposure time for diffraction at each *T*/RH setting was 4 min at the NSLS and 30−180 min at Rice. The diffraction pattern was stable during these exposure times. No streaks or elongated peaks were observed, indicating that the underlying structure of the sample was stable during the measurement.

RESULTS AND DISCUSSION

Figure 1 shows the four diffraction patterns observed in the range of temperature 20−65 °C, humidity 35−100% RH, and the DOPC/DOPE ratios 1/0, 3/1, 2/1, 1/1, 1/2, 1/3, and 0/1. At a very small incident angle, the coordinates of the diffraction pattern on the area detector are approximately in proportion to the reciprocal spacing. The vertical coordinate is perpendicular to the substrate surface. The horizontal coordinate is proportional to the magnitude of the in-plane component of the reciprocal vector. (Note that the crystalline domains were randomly oriented around the vertical.) The pattern of Figure 1a corresponds to a lamellar lattice (L_α),

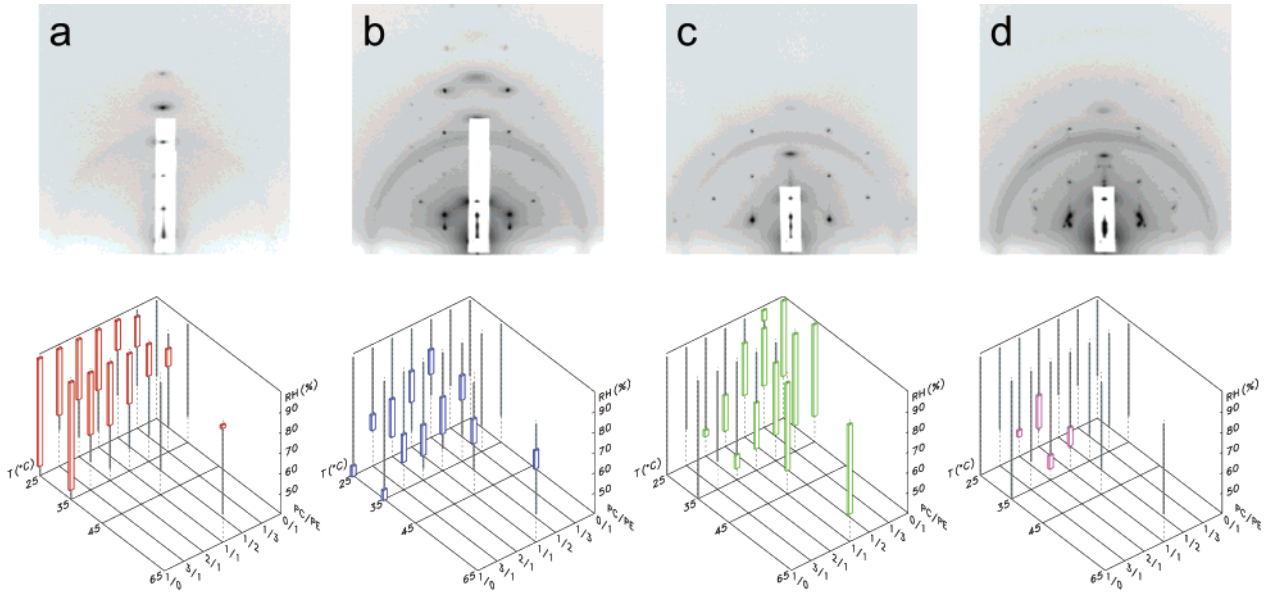

FIGURE 1: Phases of DOPC/DOPE mixtures identified by diffraction patterns. The X-ray diffraction patterns were recorded on an area detector at a fixed incident angle such that the coordinates on the area detector are approximately in proportion to the reciprocal spacing. The vertical coordinate is perpendicular to the substrate surface. The horizontal coordinate is proportional to the magnitude of the in-plane component of the reciprocal vector. (The crystalline domains were randomly oriented around the vertical.) All four patterns are on the same scale; the red bar shown in (a) represents 1.0 nm^{-1}. The white strip in each image was the shadow of an X-ray attenuator. The dark rings were due to the kapton windows on the sample chamber. The images are diffraction patterns of (a) a lamellar structure corresponding to the L_α phase, (b) a rhombohedral structure (space group $R\bar{3}$) designated as the R phase, (c) a two-dimensional hexagonal structure (space group *P*6) corresponding to the inverted hexagonal (H_{II}) phase, and (d) a two-dimensional distorted hexagonal structure (space group *P*2) designed as the $H_{II\delta}$ phase. Below each image, we show the temperature (*T*), the ambient relative humidity (RH), and the DOPC/DOPE ratio of the sample where each phase was detected (the phase symbols are L for L_α, R for R, H for H_{II}, and D for $H_{II\delta}$). The experiment was performed by varying the humidity in steps of 3% RH at a fixed temperature. The vertical thick gray lines indicate the range of RH within which the measurement was taken.

Figure 1b to a rhombohedral lattice (R), Figure 1c to a two-dimensional hexagonal lattice (H_{II}), and Figure 1d to a two-dimensional distorted hexagonal lattice ($H_{II\delta}$). The symmetry of $H_{II\delta}$ is 2D monoclinic (space group *P*2), but it is more useful to view it as a distorted hexagonal. Such a phase has not been reported before and appears not to exist in single-component lipids (*17*, *18*). A rhombohedral phase of lipid was first discovered by Luzatti's group (*16*) but not between L_α and H_{II}. Its unit cell structure is also different from what is seen here. The reason the R and $H_{II\delta}$ phases were not detected previously in the DOPC−DOPE system is not clear. The main difference between the previous experiments (*4*, *5*, *7*, *11*, *12*) and ours is in the sample preparation, i.e., powder vs substrate-supported samples. In our experiment the hexagonal planes of the R phase and the lipid cylinders of the hexagonal phase laid parallel to the substrate. Perhaps the substrate helped in stabilizing large domains of these new phases, making them easier to be detected.

The R phase appeared to be an equilibrium state, unlike the cubic phase of DOPE observed by Shyamsunder et al. (*19*) at ∼4 °C that was considered metastable. This cubic phase emerged only after the DOPE sample was subjected to a thermal cycle between −5 and 15 °C, repeated for hundreds of times (*19*). On the contrary, the phase diagrams shown in Figures 1 and 2 were reproduced repeatedly without any special treatment given to the samples. The $H_{II\delta}$ phase also appeared to be an equilibrium state, except its diffraction pattern seemed most of the time accompanied by a small minority of either the R phase or the regular H_{II} phase (see the legend of Figure 2).

An R phase between an L_α and an H_{II} phase was first found by two of us (*9*, *10*) in DPhPC by the same diffraction technique. The electron density distribution of its unit cell was constructed from the diffraction pattern (*9*, *10*). Its structure can be viewed as the consequence of an osmotic pressure (due to dehydration) on a lamellar phase that causes neighboring bilayers to make local contacts and the subsequent merging of two contacting monolayers, making the previously separated monolayers continuous via an hourglass-shaped structure, or a stalk, as theoretically expected (*6*−*8*). The R phase reported by Luzzati's group was described as a stack of hexagonal networks of inverted tubes of lipid (*16*). The topology of Luzzati's structure is the same as ours, but the two differ in the unit cell structure. The R phase of DOPC−DOPE mixtures is similar to that of the DPhPC. This is the intermediate structure that has been theoretically expected to be between a lamellar phase and a hexagonal phase. However, as shown in the phase diagrams (Figures 1 and 2), not all L_α−H_{II} transitions have an intermediate R phase. Pure DOPC has only lamellar and rhombohedral phases for humidities above 35% RH. As the fraction of DOPE increases in the mixture, the R phase appears in higher humidities and the hexagonal phases H_{II} and $H_{II\delta}$ appear on the low hydration side. The R phase only appears in the DOPC/DOPE mixtures with the molar ratio greater than ∼1/2. Below that ratio, the R phase is absent, and the lamellar phase transforms directly to the hexagonal phase. Interestingly, the pattern of the phase diagram remains the same at higher temperatures, except that the same pattern shifts to lower DOPC/DOPE ratios. For example, the phase diagram of 1/1 DOPC/DOPE at 65 °C is similar to that of 1/2 DOPC/DOPE at 35 °C (see Figure 2). Conversely, the phase diagram of pure DOPE at low temperatures observed by Gawrisch et al. (*12*) is similar to that of 1/3 DOPC/DOPE in Figure 2;

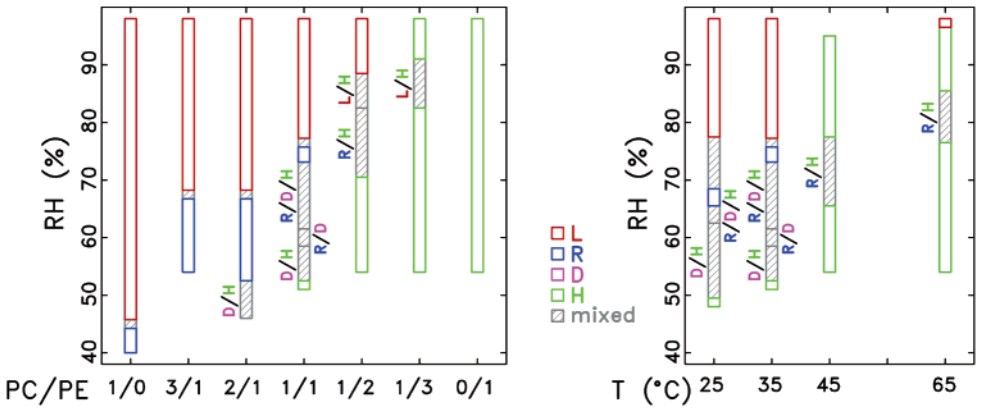

FIGURE 2: Phase diagram of DOPC/DOPE mixtures. Each sample was measured twice at each *T*/RH setting, once by increasing and the other time by decreasing the hydration to the set point. The phase boundaries depend somewhat on the direction of hydration change. Thus some part of the observed mixed regions might contain metastable structures that do not represent the true equilibrium phases. These approximate phase diagrams have been reproduced by repeated measurements with independently prepared samples. (Left) Phase diagram at 35 °C. (Right) Phase diagram of 1/1 DOPC/DOPE at different temperatures. Note that the effect of raising the temperature in the phase diagram at the right is similar to lowering the DOPC/DOPE ratio in the phase diagram at the left.

i.e., there is a L_α phase between the high RH and the low RH H_{II} phases. Thus, roughly speaking, increasing temperature is equivalent to increasing DOPE in the mixture, and decreasing temperature is equivalent to increasing DOPC in the mixture. It is an important observation that a rhombohedral phase may not exist in full hydration. The R phase seems only to appear on the dehydrated side of a lamellar phase. Similarly, the process leading to a fusion event is the removal of the water molecules between two bilayers. A stalk intermediated state is supposed to emerge from such a locally dehydrated condition.

Another new feature in the phase diagram is the distorted hexagonal phase. Significantly, the discovery of this phase alters the concept of the bending energy for a mixed-lipid monolayer. Conventionally, a lipid monolayer is described as having a spontaneous curvature C_o, and its bending energy is given as an integral over the area A, $\int\kappa(C - C_o)^2\, dA$, where κ is the bending rigidity and C the actual mean curvature of the monolayer (*11*, *20*). We now realize that the spontaneous curvature may not be a constant in a mixed-lipid monolayer. Figure 3 shows the reciprocal vectors $\mathbf{b}_1$ ($b_1 \cos\gamma$, $b_1 \sin\gamma$) and $\mathbf{b}_2$ (0, b_2) for the distorted hexagonal pattern (Figure 1d) and the corresponding crystal axes $\mathbf{a}_1$ (a_1, 0) and $\mathbf{a}_2$ ($-a_2 \cos\gamma$, $a_2 \sin\gamma$). In a regular hexagonal pattern (Figure 1c) we have $\gamma = \pi/3$, $b_1 = b_2$, and $a_1 = a_2$. One can transform a regular hexagonal lattice into a distorted hexagonal lattice by the transformation $(x,y) \rightarrow (x - \beta y, \alpha y)$, where α and β are obtained from $\alpha a_1 \sin(\pi/3) = a_2 \sin\gamma$ and $\beta a_1 \sin(\pi/3) = a_2 \cos\gamma - a_1 \cos(\pi/3)$. For example, if a regular hexagonal phase contains circular cylinders (*21*) of lipid with a cross section described as $a(\cos t, \sin t)$, $t = 0$ to 2π, a distorted hexagonal phase could contain distorted cylinders with a cross section given by $a'(\cos t - \beta \sin t, \alpha \sin t)$, where we allow rescaling of a'. The former has a constant curvature $C = 1/a$, and the latter $C = (\alpha/a')\{\sin^2 t + 2\beta \sin t \cos t + (\alpha^2 + \beta^2)\cos^2 t\}^{-3/2}$. The shape of the cross section of the lipid cylinders in a regular hexagonal phase is not known exactly but is most likely between circular and hexagonal (*21*). It is obvious that energetically a constant spontaneous curvature favors a regular hexagonal phase. Thus the appearance of a distorted hexagonal phase implies that the local spontaneous curvature varies around the lipid cylinder. This could happen only if the lipids had demixed from the average stoichiometric ratio, so that the local DOPC/DOPE ratio is not uniform around the cross section. Why some of the hexagonal phases are distorted but the others are regular (see Figure 2) will need to be investigated further.

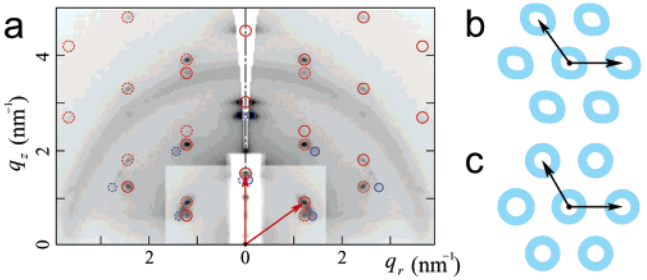

FIGURE 3: Lattice of the distorted hexagonal phase. (a) The diffraction peaks of 1/1 DOPC/DOPE at 25 °C and 56% RH are on a 2D monoclinic lattice (space group *P*2) marked by solid red circles defined by the reciprocal vectors $\mathbf{b}_1$ (1.51 cos γ, 1.51 sin γ) and $\mathbf{b}_2$ (0, 1.51) nm^{-1}, where $\gamma = 53.8°$ is the angle between the two vectors. The peaks marked by dotted red circles are the mirror image of those marked by solid red circles. The appearance of the mirror image is due to the crystalline domains being randomly oriented in the plane of the substrate. (There is also a minority distorted hexagonal phase whose plane is not parallel to the substrate, as marked in blue.) (b) The corresponding crystal axes $\mathbf{a}_1$ (4.16, 0) and $\mathbf{a}_2$ ($-4.16 \cos\gamma$, $4.16 \sin\gamma$) nm. (c) A regular hexagonal lattice, for comparison.

In molecular biology the membrane fusion problem is unique in having a very active theoretical input (*7*, *14*, *15*, *22*−*29*). This is due to the recognition that the functions of fusion proteins can only be understood in terms of their couplings with the free energy pathway of lipid conformation changes (*1*, *2*). However, as the long succession of recalculations for the stalk energy (*7*, *13*−*15*, *22*, *23*, *25*, *26*) shows, there has been a lack of experimental constraints on the theoretical calculations. Here the finding of the R phase between L_α and H_{II} confirms the previously speculated stalk hypothesis. At the same time the phase diagram of the R phase indicates an unforeseen constraint for the formation of stable stalks. A mixture of DOPC and DOPE modulates the spontaneous curvature to a value between a small C_o of DOPC and a large C_o of DOPE. Apparently, an R phase is compatible only with a certain range of C_o not exceeding that of 1/2 DOPC/DOPE. The existence of distorted hex-

agonal phase implies that a monolayer consisting of multiple lipid components may demix, or adjust its local spontaneous curvature to achieve energy minimum, under stress. This suggests the possibility that the energies of the intermediate states of membrane fusion may be lowered by this degree of freedom. These experimental facts will need to be incorporated into theoretical considerations henceforth.

REFERENCES

1. Lentz, B. R., Malinin, V., Haque, M. E., and Evans, K. (2000) Protein machines and lipid assemblies: current views of cell membrane fusion, *Curr. Opin. Struct. Biol. 10*, 607−615.
2. Blumenthal, R., Claque, M. J., Durell, S. R., and Epand, R. M. (2003) Membrane fusion, *Chem. Rev. 103*, 53−69.
3. Hui, W. W., Stewart, T. P., Boni, L. T., and Yeagle, P. L. (1981) Membrane fusion through point defects in bilayers, *Science 212*, 912−923.
4. Gruner, S. M. (1989) Stability of lyotropic phases with curved interfaces, *J. Phys. Chem. 93*, 7562−7570.
5. Ellens, H., Siegel, D. P., Alford, D., Yeagle, P. L., Boni, L., Lis, L. J., Quinn, P. J., and Bentz, J. (1989) Membrane fusion and inverted phases, *Biochemistry 28*, 3692−3730.
6. Siegel, P. D., and Epand, R. M. (1997) The mechanism of lamellar-to-inverted hexagonal phase transitions in phosphatidylethanolamine: implications for membrane fusion mechanisms, *Biophys. J. 73*, 3089−3111.
7. Siegel, D. P. (1999) The modified stalk mechanism of lamellar/inverted phase transitions and its implications for membrane fusion, *Biophys. J. 76*, 291−313.
8. Ortiz, A., Killian, J. A., Verkleij, A. J., and Wilschut, J. (1999) Membrane fusion and the lamellar-to-inverted-hexagonal phase transition in cardiolipin vesicle systems induced by divalent cations, *Biophys. J. 77*, 2003−2014.
9. Yang, L., and Huang, H. W. (2002) Observation of a membrane fusion intermediate structure, *Science 297*, 1877−1879.
10. Yang, L., and Huang, H. W. (2003) A rhombohedral phase of lipid containing a membrane fusion intermediate structure, *Biophys. J. 84*, 1808−1817.
11. Rand, R. P., Fuller, N. L., Gruner, S. M., and Parsegian, V. A. (1990) Membrane curvature, lipid segregation, and structural transitions for phospholipids under dual-solvent stress, *Biochemistry 29*, 76−87.
12. Gawrisch, K., Parsegian, V. A., Hajduk, D. A., Tate, M. W., Gruner, S. M., Fuller, N. L., and Rand, R. P. (1992) Energetics of a hexagonal-lamellar-hexagonal phase transition sequence in dioleoylphosphatidylethanolamine membranes, *Biochemistry 31*, 2856−2864.
13. Lentz, B. R., Siegel, D. P., and Malinin, V. (2002) Filling potholes on the path to fusion pores, *Biophys. J. 82*, 555−557.
14. Markin, V. S., and Albanes, J. P. (2002) Membrane fusion: stalk model revisited, *Biophys. J. 82*, 693−712.
15. May, S. (2002) Structure and energy of fusion stalks: the role of membrane edges, *Biophys. J. 83*, 2969−2980.
16. Ludtke, S., He, K., and Huang, H. W. (1995) Membrane thinning caused by magainin 2, *Biochemistry 34*, 16764−16769.
17. Luzzati, V., Gulik-Krzywicki, T., and Tardieu, A. (1968) Polymorphism of lecithins, *Nature 218*, 1031−1034.
18. Tardieu, A., Luzatti, V., and Reman, F. C. (1973) Structure of polymorphism of the hydrocarbon chains of lipids: a study of lecithin-water phases, *J. Mol. Biol. 75*, 711−733.
19. Shyamsunder, E., Gruner, S. M., Tate, M. W., Turner, D. C., and So, P. T. C. (1988) Observation of inverted cubic phase in hydrated dioleoylphosphatidylethanolamine membranes, *Biochemistry 27*, 2332−2336.
20. Helfrich, W. (1973) Elastic properties of lipid bilayers: theory and possible experiments, *Z. Naturforsch. 28C*, 693−703.
21. Turner, D. C., and Gruner, S. M. (1992) X-ray diffraction reconstruction of the inverted hexagonal (H_{II}) phase in lipid-water systems, *Biochemistry 31*, 1340−1355.
22. Markin, V. S., Kozlov, M. M., and Borovjagin, V. L. (1984) On the theory of membrane fusion. The stalk mechanism, *Gen. Physiol. Biophys. 3*, 361−377.
23. Siegel, D. P. (1993) Energetics of intermediates in membrane fusion: comparison of stalk and inverted micellar intermediate mechanisms, *Biophys. J. 65*, 2124−2140.
24. Chizmadzhev, Y. A., Kuzmin, P. I., Kumenko, D. A., Zimmerberg, J., and Cohen, F. S. (2000) Dynamics of fusion pores connecting membranes of different tensions, *Biophys. J. 78*, 2241−2256.
25. Kuzmin, P. I., Zimmerberg, J., Chizmadzhev, A., and Cohen, F. S. A. (2001) Quantitative model for membrane fusion based on low-energy intermediates, *Proc. Natl. Acad. Sci. U.S.A. 98*, 7235−7240.
26. Kozlovsky, Y., and Kozlov, M. M. (2002) Stalk model of membrane fusion: solution of energy crisis, *Biophys. J. 82*, 882−895.
27. Chanturiya, A., Scaria, P., Kuksenok, O., and Woodle, M. C. (2002) Probing the mechanism of fusion in a two-dimensional computer simulation, *Biophys. J. 82*, 3072−3080.
28. Kozlovsky, Y., Chernomordik, L. V., and Kozlov, M. M. (2002) Lipid intermediates in membrane fusion: formation, structure, and decay of hemifusion diaphragm, *Biophys. J. 83*, 2634−2651.
29. Marrink, S.-J., and Tieleman, D. P. (2002) Molecular dynamics simulation of spontaneous membrane fusion during a cubic-hexagonal phase transition, *Biophys. J. 83*, 2386−2392.

BI0344836